Molecular Physics

Breakdown of the Franck-Condon approximation in N_2
Canton, S.E., J.D. Bozek, N. Berrah

Circular dichroism in K-shell ionization from fixed-in-space CO and N_2 molecules
Jahnke, T., Th. Weber, A.L. Landers, A. Knapp, S. Schössler, J. Nickles, S. Kammer, O. Jagutzki, L. Schmidt, A. Czasch, T. Osipov, E. Arenholz, A.T. Young, R. Díez Muiño, D. Rolles, F.J. García de Abajo, C.S. Fadley, M.A. Van Hove, S.K. Semenov, N.A. Cherepkov, J. Rösch, M.H. Prior, H. Schmidt-Böcking, C.L. Cocke, R. Dörner

Experimental evidence of a dynamic Jahn-Teller effect in $D_{3d}C_{60}^{+}$
Canton, S.E., A. J. Yencha, M.C.A. Lopes, E. Kukk, J.D. Bozek, G. Snell, N. Berrah

Multi-atom resonant photoemission effects from solid surfaces and free molecules
Mannella, N., B.S. Mun, S.-H. Yang, A.W. Kay, F.J. Garcia de Abajo, E. Arenholz, A.T. Young, Z. Hussain, H. Wang, O. Hemmers, D.W. Lindle, M.A. Van Hove, C.S. Fadley

Shallow and deep core level ionic fragmentation of the CCl_4 molecule
Santos, A.C.F., J.B. Maciel, M.M. Sant' Anna, K.T. Lung, J. Cotter, W. Stolte, G.G.B. de Souza

Soft x-ray emission spectroscopy of ions in solution
Augustsson, A., J.-H. Guo, D. Spandberg, K. Hermansson, J. Nordgren

Spin-resolved electron spectroscopy of carbonyl sulphide
Turri, G., G. Snell, B. Langer, M. Martins, E. Kukk, P. Langhoff, N. Berrah

Vibrationally resolved resonant Auger spectroscopy of formaldehyde at the C $1s^{-1}$ π^* resonance
Bozek, J.D., S.E. Canton, E. Kukk, N. Berrah

BREAKDOWN OF THE FRANCK-CONDON APPROXIMATION IN N_2

S.E. Canton[1,2], J.D. Bozek[1] and N. Berrah[2]
[1] Lawrence Berkeley National Laboratory, Advanced Light Source,
University of California, Berkeley CA 94720.
[2] Department of Physics, Western Michigan University, Kalamazoo MI 49008.

INTRODUCTION

When a molecular electron is excited or ionized, it moves in a different charge distribution exerting in turn a different force on the nuclei. The nuclei respond by breaking into stronger vibrations. Electronic transitions are accompanied by vibrational transitions, which are called vibronic. The determination of which vibrations are stimulated is based on the view that nuclei move much faster than electrons, and so the rearrangement occurs in a virtually static nuclear frame. The Franck-Condon principle is the approximation that the nuclear conformation readjusts after the electronic transition, and not during it. The most probable conformation of the molecule when the transition begins is at the nuclei equilibrium position. At the end of the transition, the nuclei are still in their original position and this is the origin of the term vertical transition. The intensity of a transition between vibronic states depends on the magnitude of the transition moment. In the frame of the Franck-Condon approximation, it can be written as:

$$<\varepsilon'\nu'|\mu|\varepsilon\nu> = \mu_{\varepsilon'\varepsilon} * S_{\nu\nu'}$$

$S_{\nu\nu'}$ is the so-called Franck-Condon factor. It can then be seen that the ratio between two vibrational levels in the same electronic band should be constant.

Vibrational level intensity ratios as a function of photon energy have been determined in the valence spectrum of N_2 from 20-400 eV using photoelectron spectroscopy. Results for the B state show a large deviation from the Franck-Condon approximation and qualitatively agree with some recent fluorescent results [1,2].

EXPERIMENT

The experiment was conducted on beamline 10.0.1 at the ALS using a Scienta SES-200 hemispherical analyzer. The transmission function of the spectrometer was accounted for before extracting the gaussian fits of the peaks areas.

RESULTS

Vibrationally resolved photoelectron cross-sections of simple molecules were obtained close to threshold to explore the dynamical effects of shape resonances and Cooper minima on photoionization cross sections using 2nd generation light sources. Experimental resolution limitations made it impossible to extend those measurements beyond 40 eV. Recently, however, a recent experiment [1,2] was carried out to access vibrationally resolved photoionization data over a much wider spectral range using dispersed fluorescence from the residual photoion. Vibrational level population distributions of N_2^+ photoions in the $B^2\Sigma_u^+$ electronic state were probed by detecting the fluorescence emitted as they decayed into the $X^2\Sigma_g^+$ ionic state. Results for the B state shows a large deviation from the Franck-Condon approximation. We report in this work a *direct* similar study of this effect using photoelectron spectroscopy of these vibrational

levels population was conducted in the present experiment. Vibrational level intensity ratios as a function of photon energy were determined from 20-400 eV and are displayed in Fig.1 for the X state, in Fig.2 for the A state and in Fig.3 for the B state. Results for the B state show a large deviation from the Franck-Condon approximation consistent with the fluorescent results.

A complete analysis of the results is currently underway.

REFERENCES

[1] Rao et al, Phys. Rev. Lett. **76**, 2666 (1996).
[2] Prof. E. Poliakoff (private communication).

ACKNOWLEDGEMENT

Prof E. Poliakoff is greatly acknowledged for making the fluorescence data available.

This work was funded by the Department of Energy, Office of Science, Basic Energy Sciences, Chemical and Material Science Division, under the contract No. DE-AC03-76SF00098.

Principal investigator: Nora Berrah, Physics Dept., Western Michigan University, 616-387-4955, berrah@wmich.edu.

Fig. 1 Branching ratio v_1/v_0 for the X state as a function of photon energy.

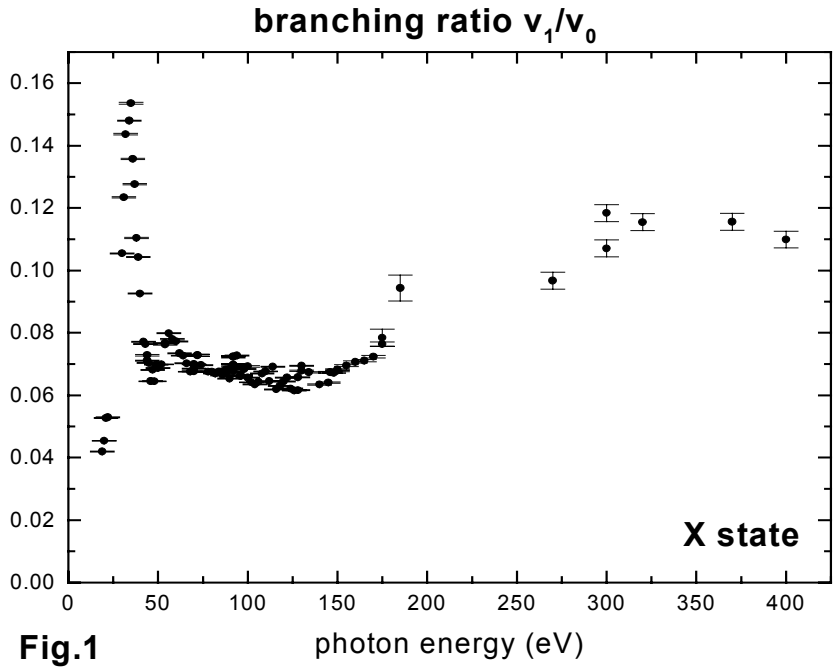

Fig.1

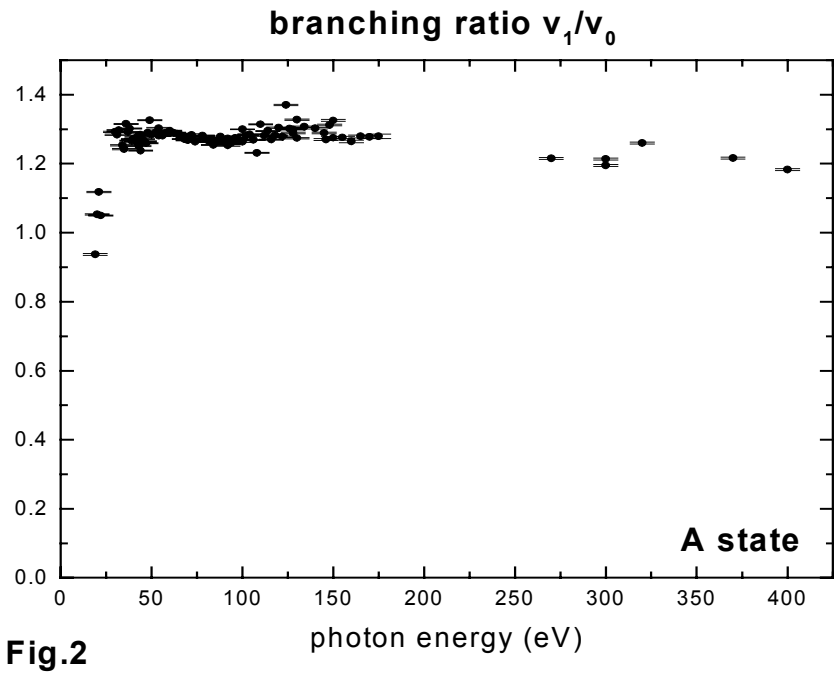

Fig.2 Branching ratio v_1/v_0 for the A state as a function of photon energy.

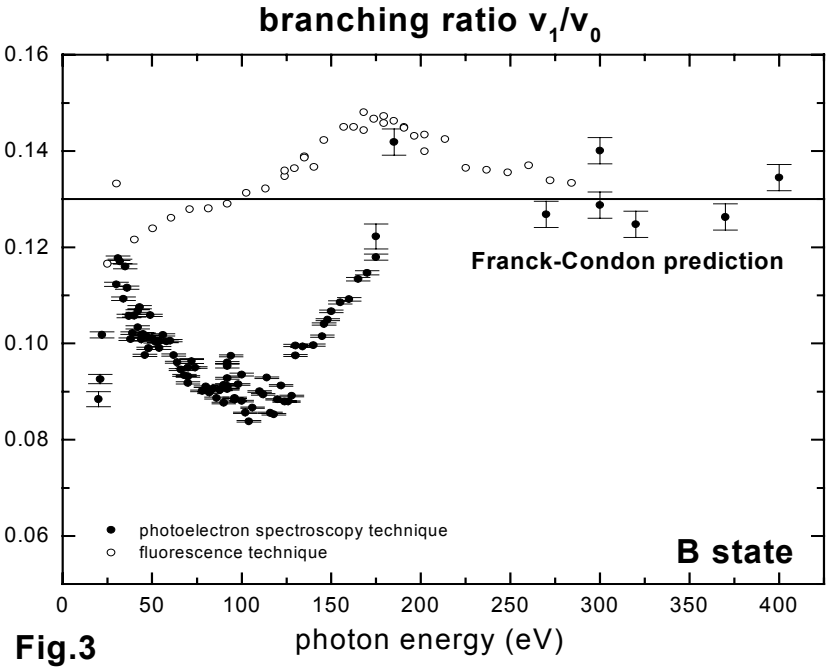

Fig.3 Branching ratio v_1/v_0 for the B state as a function of photon energy compared with fluorescence data (open circles).

Circular Dichroism in K-shell Ionization from Fixed-in-Space CO and N_2 Molecules

T. Jahnke[1], Th. Weber[1], A.L. Landers[2], A. Knapp[1], S. Schössler[1], J. Nickles[1], S. Kammer[1], O. Jagutzki[1], L. Schmidt[1], A. Czasch[1], T. Osipov[3], E. Arenholz[4], A.T. Young[4], R. Díez Muiño[5,6], D. Rolles[5], F.J. García de Abajo[5], C.S. Fadley[5,7], M.A. Van Hove[4,5,7], S.K. Semenov[8], N.A. Cherepkov[8], J. Rösch[9], M.H. Prior[9], H. Schmidt-Böcking,[1] C.L. Cocke,[3] and R. Dörner[1]

[1] Institut für Kernphysik, University Frankfurt, August-Euler Str 6, D-60486 Frankfurt Germany
[2] Dept. of Physics, Western Michigan Univ., Kalamazoo, MI 49008, USA
[3] Dept. of Physics, Kansas State Univ, Cardwell Hall, Manhattan, KS 66506, USA
[4] Advanced Light Source, Ernest Orlando Lawrence Berkeley National Laboratory, University of California, Berkeley, California 94720, USA
[5] Materials Sciences Division, Ernest Orlando Lawrence Berkeley National Laboratory, University of California, Berkeley, California 94720, USA
[6] Donóstia International Physics Center, P. Manuel de Lardizabal 4, 20018 San Sebastián, Spain
[7] Department of Physics, University of California, Davis, CA 95618, USA
[8] State University of Aerospace Instrumentation, 190000 St. Petersburg, Russia
[9] Chemical Sciences Division, Ernest Orlando Lawrence Berkeley National Laboratory, University of California, Berkeley, California 94720, USA

INTRODUCTION

This project studies photoemission (photoionization) from "fixed-in-space" molecules, comparing measured angular distributions with theory. In particular, strong circular dichroism in angular distribution (CDAD) is measured for CO and N_2, which is explained by calculations performed both in the multiple-scattering and random-phase-approximation formalisms. The new CDAD measurements, together with earlier results with linearly polarized photons [1,2], constitute the most complete description of K-shell photoemission from a free diatomic molecule. They provide benchmark tests of theoretical methods that are indispensable, for example, in the interpretation of photoemission and photoelectron diffraction data from solids.

METHODS

The present experiment was performed using COLTRIMS (Cold Target Recoil Ion Momentum Spectroscopy [3]) at elliptically polarized undulator beamline 4.0.2 of the Advanced Light Source. The resolution for the photoelectron ranges from 1-3 eV depending upon its energy; this is sufficient to discriminate the direct K-shell photoelectron from the Auger and satellite shake up electrons. In the analysis we have used for CO only the $C^+ + O^+$ decay channel with a kinetic energy release KER > 10.2 eV [2], and for N_2 all ions from the $N^+ + N^+$ decay channel.

The calculations for CO are performed in a one-electron model using multiple scattering theory in non-spherical self-consistent potentials (MSNSP) [4] using the experimental values of the electron energy. The molecular ionic potential is split into two touching roughly hemispherical cells in which the full self-consistent potential is present. This allows us to include regions of space neglected by standard multiple scattering theory, and to avoid the usual spherical symmetrization of the potentials around each atomic scattering center. The inclusion of non-spherical effects has been found to be crucial in the calculation of the photoelectron angular distributions for kinetic energies of the electron lower than approximately 30 eV [3].

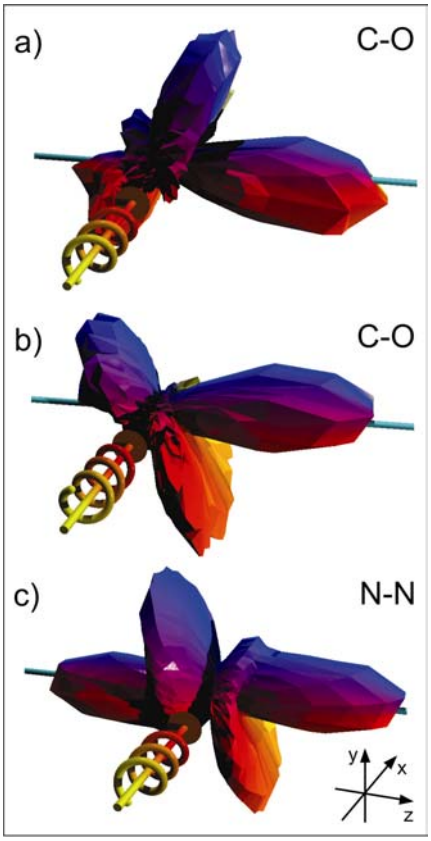

Figure 1. (a) and (b) -- Angular distributions of C(1s) photo-electrons (10 eV kinetic energy, on shape resonance) emitted from a CO molecule by absorption of left and right circularly polarized photons. The sense of rotation of the polarization vector is indicated by the spiral, where the photon propagation vector lies along the + x-axis (i.e., into the page) in all cases. The molecule is aligned along the z-axis, with the carbon atom at negative z in panels (a) and (b). Each vertex of the three-dimensional shape represents one data point. The data have not been smoothed, with the maximum corresponding to about 1000 counts. (c) -- Analogous distribution of N(1s) photoelectrons (9 eV, on resonance) from N_2.

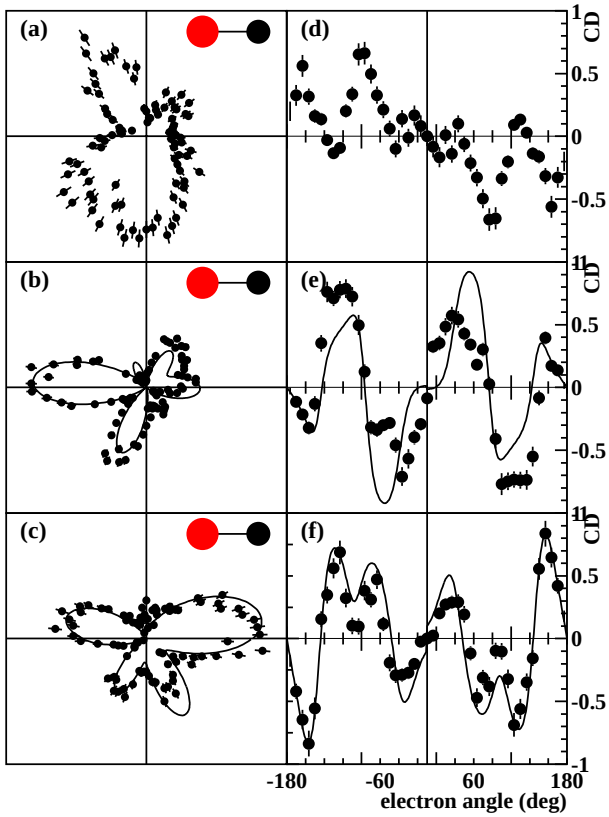

Figure 2. (a-c) Angular distribution of C(1s) photo electrons emitted from a CO molecule by absorption of right circularly polarized photons where the propagation vector of the light is into the page. The molecule lies along the horizontal axis as indicated, and both electrons and molecules lie within 10 degrees of the plane of the page. The electron energies are (a) 1.6, (b) 10.0 and (c) 24.6 eV. Panels (d-f) show the corresponding circular dichroism as defined in the text. Electron angle 0 corresponds to the direction of the carbon. Full lines: Theoretical multiple scattering calculations for the two higher energies, convoluted with the experimental resolution.

For N_2, the calculations take many-electron correlations into account in the Random Phase Approximation (RPA) [5,6]. In this approach, the non-spherical relaxed core Hartree-Fock potential is used as the zero order approximation for the photoelectron wave functions, and the coupling between the 1σ-g and 1σ-u channels is included within the RPA method.

RESULTS

More quantitatively, Fig. 2 shows the photoelectron angular distribution from CO in the y-z-plane (perpendicular to the photon propagation) where CDAD is strongest. The molecule lies along the horizontal axis, as shown in the schematic, and the photon propagation vector is into the page. The electron energies are 1.6, 10.0 and 24.6 eV. The carbon-K σ shape resonance

results in a maximum of the cross section at around 10 eV (306 eV photon energy). The right panels show the CDAD defined as:

$$CDAD = (\sigma_{RCP} - \sigma_{LCP}) / (\sigma_{RCP} + \sigma_{LCP})$$

The theoretical calculations corresponding to the measurements are shown in Fig. 2 by the solid lines, using the multiple-scattering formalism: good overall agreement between experiment and theory is found.

Similar agreement between experiment and theory was obtained (not shown) for N_2, in which case the random-phase-approximation approach was used.

ACKNOWLEDGMENTS

This work was supported in part by BMBF and DFG. R.D. was supported by the Heisenberg Programm der DFG, the Alexander von Humboldt and the Adolf Messer Stiftung. Th.W. thanks Graduiertenförderung des Landes Hessen for financial support. We thank Roentdek GmbH (www.Roentdek.com) for support with the delayline detectors. S.K.S. and N.A.C. acknowledge the financial support of the INTAS-RFBR grant (IR-97-471). R.D. acknowledges many enlightening discussions with J. Berakdar on the relationship of CDAD to phase information.

REFERENCES

1. A. Landers, T. Weber, I. Ali, A. Cassimi, M. Hattass, O. Jagutzki, A. Nauert, T. Osipov, A. Staudte, M.H. Prior, H. Schmidt-Böcking, C.L. Cocke, and R. Dörner, Phys. Rev. Lett. **87**, 013002.
2. T. Weber, O. Jagutzki, M. Hattass, A. Staudte, A. Nauert, L. Schmidt, M. Prior, A. Landers, A. Bräuning-Demian, H. Bräuning, et al, J. Phys. **B34**, 3669 (2001).
3. R. Dörner, V. Mergel, O. Jagutzki, L. Spielberger, J. Ullrich, R. Moshammer and H. Schmidt-Böcking, Physics Reports **330**, 96 (2000).
4. R. Díez Muiño, D. Rolles, F.J. García de Abajo, F. Starrost, W. Schattke, C.S. Fadley and M.A. Van Hove, J. of Electr. Spectr. and Rel. Phenom. **99**, 114 (2001).
5. S.K. Semenov, N.A. Cherepkov, G.H. Fecher and G. Schönhense, Phys. Rev. **A61**, 032704 (2000).
6. N.A. Cherepkov, S.K. Semenov, Y. Hikosaka, K. Ito, S. Motoki and A. Yagishita, Phys. Rev. Lett. **84**, 250 (2000).

This work was supported by the Director, Office of Science, Office of Basic Energy Sciences, Geo-, Bio-, Chemical and Materials Sciences Divisions, of the U.S. Department of Energy under Contract No. DE-AC03-76SF00098.

Principal investigator: Michel A. Van Hove, Advanced Light Source and Materials Sciences Division, Ernest Orlando Lawrence Berkeley National Laboratory. Email: MAVanHove@lbl.gov. Telephone: 510-486-6160.

Experimental evidence of a dynamic Jahn-Teller effect in D_{3d} C_{60}^{+}

S.E. Canton[1,2], A.J. Yencha[4], M.C.A. Lopes[5],
E. Kukk[3], J.D. Bozek[1] G.Snell[2] and N. Berrah[2]
[1] Lawrence Berkeley National Laboratory, Advanced Light Source,
University of California, Berkeley CA 94720.
[2] Department of Physics, Western Michigan University, Kalamazoo MI 49008.
[3] Department of Physical Sciences, Oulu University, Linnanmaa, Oulu FIN-90570, Finland.
[4] Department of Chemistry, State University of New-York at Albany, Albany NY 122222
[5] Departmento de Fisica, ICE, Universidade Federal de Juiz de Fora, Juiz de Fora-MG,
CEP 36036-330 Brazil.

INTRODUCTION

Since its discovery in 1985, C_{60} has been the subject of intense studies. Most of its astonishing properties can be explained by its particular electronic structure. However, very little is known about C_{60}^{+}, which is of great interest for astrophysics and solid state physics. Characteristics as fundamental as the shape of the cation are still under debate. Because of its high symmetry, C_{60}^{+} experiences a Jahn-Teller distortion and the Born-Oppenheimer approximation commonly used to obtained adiabatic potential energy surfaces is not applicable in this case. A recent analytical model [2] predicts different equilibrium geometry depending on the electron-phonon coupling strength. The number of vibronic states is shown to be directly correlated to the geometry. We have recently measured the valence photoelectron spectrum of C_{60}. The three-peak structure of the Highest Occupied Molecular Orbital (HOMO) is clearly resolved and strongly supports a D_{3d} geometry for C_{60}^{+} in its ground state.

EXPERIMENT

The experiment was performed on beamline 10.0.1 at the ALS. A resistively heated oven generated an effusive beam of C_{60}. The photoelectron spectra were recorded in a crossed beam configuration using a Scienta SES-200 hemispherical analyzer at the magic angle. The spectrometer was operated at 20 eV pass energy and the photon resolution was set to 10 meV.

RESULTS

Semi classical and ab-initio calculations agree to attribute H_u symmetry to the highest occupied molecular orbital (HOMO) of C_{60}. The JT active modes are then of h and g symmetry. As this outermost orbital is highly delocalized over the rigid frame of 60 carbon atoms, any distortion is supposed to be small and the resulting ionized states are going to be best described as originating from a dynamic JT effect. The corresponding static $H\otimes(h\oplus g)$ JT problem was investigated analytically [1]. Minimization of the adiabatic energy surface for this problem results in wells of either D_{5d} or D_{3d} symmetry depending on the coupling strength. The dynamic JT problem can then be solved in the tunneling regime [2] to find the I_h symmetrized combinations of the states associated with the wells. The findings are the following: if the coupling is very strong, the absolute minimum has a D_{3d} symmetry and there are 3 tunneling states of A (not degenerate), G (4 times degenerate) and H (5 times degenerate) symmetry. In the case of weaker coupling, the absolute minimum is of D_{5d} symmetry and there are 2 tunneling states of A and H symmetry.

The present analysis of the bandshape in photoelectron spectra recorded at the magic angle strongly supports the first experimental evidence of a D_{3h} equilibrium geometry. The fitting procedure with asymmetric gaussians (Fig 1). allows the extraction of 3 bands I, II and III of area in the 1:4:5 ratio, corresponding to the tunneling states. An attempt to model the envelope with only 2 underlying peaks fails to reproduce the overall shape and doesn't give the areas in the 1:5 ratio. This rules out the possibility of a D_{5h} geometry predicted by an INDO calculation [3] and raises the question of the validity of the perturbative approach often used to derive some of the properties of this material, as the D_{3h} geometry is the signature of a strong electron-phonon interaction [2].

REFERENCES

[1] A. Ceulemans, P.W. Fowler, J. Chem. Phys. **93**, 1221 (1990).
[2] C. P. Moate et al, J. Phys. Condens. Matter **9**, 6049 (1997).
[3] R.D. Bendale et al, Chem. Phys. Lett., **194**, 467 (1992).

ACKNOWLEDGEMENTS

M.C.A. Lopes gratefully acknowledges financial support from CNPq (Brazil)
This work was funded by the Department of Energy, Office of Science, Basic Energy Sciences, Chemical Science Division, under the contract No. DE-AC03-76SF00098.

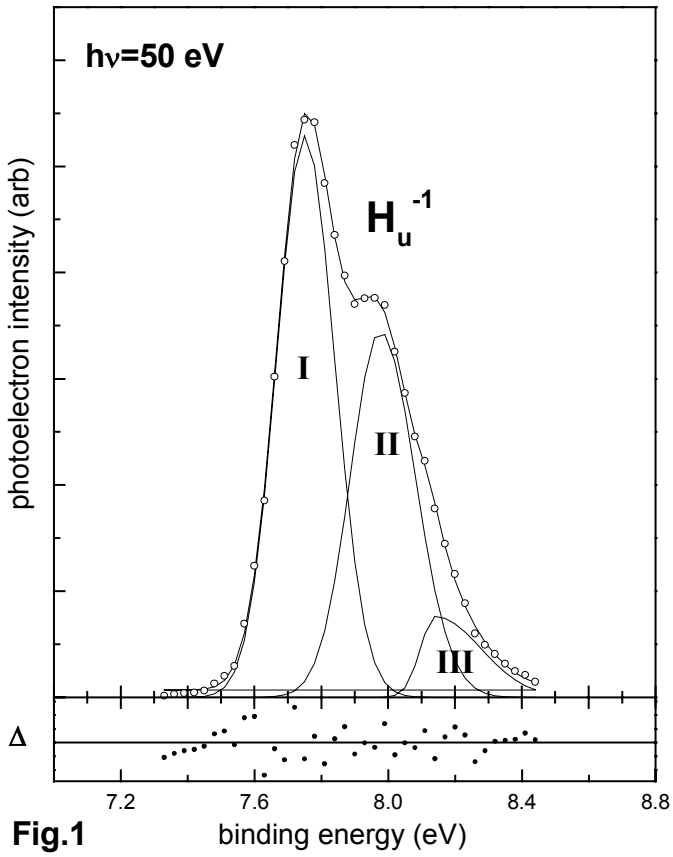

Fig.1

Fig.1: Fit of the HOMO band by three asymmetric gaussians. Δ indicates the difference between the data points and the fit.

This work was supported by the Director, Office of Science, Office of Basic Energy Sciences, of the U.S. Department of Energy under Contract No. DE-AC03-76SF00098.

Principal investigator: Nora Berrah, Western Michigan University. Email: berrah@wmich.edu.
Telephone: 616-387-4955.

Multi-Atom Resonant Photoemission Effects from Solid Surfaces and Free Molecules

N. Mannella[1,2], B.S. Mun[1,2], S.-H. Yang[2], A.W. Kay[1,2,#],F.J. Garcia de Abajo[1,3], E. Arenholz[4], A.T. Young[4], Z. Hussain[4], H. Wang[5], O. Hemmers[5], D.W. Lindle[5], M.A. Van Hove[1,2], and C.S. Fadley[1,2]

[1]Dept. of Physics, University of California-Davis, Davis, CA 95616
[2]Materials Sciences Division, Lawrence Berkeley National Laboratory, Berkeley, CA 94720
[3] Centro Mixto CSIC-UPV/EHU, San Sebastian, Spain
[4]Advanced Light Source, Lawrence Berkeley National Laboratory, Berkeley, CA 94720
[5]Dept. of Chemistry, University of Nevada, Las Vegas, NV 89154
[#]Present address: Intel Corporation, Portland, OR

INTRODUCTION

In prior work at the ALS, it has been pointed out that a new type of interatomic resonant photoemission effect exists, and that this effect furthermore has the potential of providing a useful probe of near-neighbor atomic identities, bonding, and magnetism [1-5]. The phenomenon has been termed multi-atom resonant photoemission (MARPE). In measuring this effect, the photoelectron intensity of a given core level from atom "A" (e.g. O 1s from MnO) is monitored while the photon energy is tuned through a strong absorption edge for a core level on another atom "B" in the sample (e.g. the Mn 2p edges in MnO). Initial observations on MnO and other metal oxides appeared to show significant entirely-positive interatomic resonant effects in photoemission of up to 100% [1]. Additional measurements in Auger emission and soft x-ray emission from MnO seemed to confirm that such effects were also present in secondary decay processes as a result of resonant enhancement of the initial O 1s core hole formation [2]. A theoretical model for these effects based on the extension of intraatomic resonant photoemission ideas to the interatomic case was also developed and compared favorably with experiment [3]. Other measurements on transition-metal compounds [6] and an adsorbate-substrate system [7a] seemed to confirm these measurements and analysis.

Subsequently, it has been realized that such experimental measurements require very careful allowance for potential detector non-linearities [4,5,7b], since the observed electron intensities (particularly inelastically scattered backgrounds) change dramatically in going over any core resonance. In particular, the detector used for several of the first MARPE studies [1,2,4-7a], the standard microchannel plate-plus-phosphor-plus-CCD camera incorporated in the Gammadata-Scienta series of electron spectrometers, exhibits not only a typical saturation effect for high countrates, but also a strong quadratic component of counting that goes above linear for low countrates. Thus, spectra obtained in this low-countrate regime, while not exhibiting any kind of saturation effect, can be artificially enhanced in intensity in passing over a core-level resonance. Methods of accurately correcting spectra for these non-linearities have been discussed [4,5,7b, and abstract by Mannella et al. in this 2001 Compendium]. When these effects are allowed for, the magnitude of the effect is reduced and the form is found to change, with the shape usually involving a negative-then-positive swing in intensity reminscent of a Fano profile in form [4,5,7b,8].

We here report more recent experimental results providing further evidence of such interatomic resonant effects in photoemission, for two very different limiting-case types of systems: a cleaved single-crystal oxide-NiO and a free molecule-SF_6. These data are discussed in terms of existing theoretical models for such MARPE effects [3,5], in particular, an x-ray optical (dielectric) approach that well describes the NiO data and a microscopic quantum mechanical model that should be useful in describing the SF_6 data.

EXPERIMENTAL PROCEDURE

The NiO measurements were performed on beamline 4.0.2 and made use of the Advanced Photoelectron Spectrometer/Diffractometer located there. Detector non-linearities were corrected for in all data presented here, using methods described elsewhere [4,5, and abstract in the 2001 Compendium]. A NiO single crystal was cleaved just before insertion into ultrahigh vacuum via a loadlock, then ion bombardment and annealing in oxygen to remove minor surface contaminant levels and assure correct stoichiometry before measurement. The incidence angle of the radiation was varied from grazing values of 5° to much higher values up to 40° (cf. experimental geometry in Figure 1(a)).

The SF_6 measurements were performed on beamline 8.0.1 and made use of a time-of-flight spectrometer described in detail elsewhere [9]. The detectors in this spectrometer are positioned in angle with respect to the incoming radiation and polarization vector such that non-dipole contributions to the angular distributions can be readily measured with high accuracy. For reference, the angular distributions of photoelectrons from a randomly oriented ensemble of free molecules is given by $d\sigma / d\Omega = (\sigma / 4\pi)\{1 + \beta P_2(\cos\Theta_e) + [\delta + \gamma \cos^2\Theta_e] \sin\Theta_e \cos\Phi_e\}$, with β the dipole asymmetry parameter and δ and γ the first-order non-dipole parameters (cf. geometry in Figure 2(a), with Φ_e being the azimuthal angle around the polarization vector $\boldsymbol{\varepsilon}$) [9].

EXPERIMENTAL RESULTS AND DISCUSSION

NiO(001): In Figure 1, we show experimental O 1s intensities from NiO as a function of photon energy and for five different x-ray incidence angles. For the lowest incidence angle of 5°, the effect of crossing the Ni 2p absorption resonances is dramatic, yielding a negative-then-positive excursion on crossing $2p_{3/2}$ whose amplitude is 75% of the intensity below the resonance. The magnitudes of these effects decreases as the incidence angle is increased, falling off to about 5% for an incidence angle of 40°.

Also shown in Figure 1 are theoretical curves based on an x-ray optical model of such effects, as discussed previously [5]. The optical constants that are key inputs for this model have been derived from concomitant partial-yield x-ray absorption measurements, with corrections for x-ray incidence angle and secondary electron takeoff angle [4], and subsequent Kramers-Kronig analysis [5]. The resulting theoretical curves are in excellent agreement with experiment for the lowest angle, and the agreement is very good for all other angles as well, although with some overprediction of the amplitudes at the higher angles. Non-zero effects are observed and predicted over the full angle range, in qualitative agreement with prior data for MnO [5]. These data thus disagree with one aspect of an earlier study of NiO by Finazzi et al. [8], in which they did not observe any sort of MARPE effect in O 1s emission from NiO; this lack of any effect appears to be due to measuring with too high an incidence angle and having insufficient statistical accuracy to resolve the small remaining effects seen, e.g. in Figures 2(e)-2(f).

We thus expect such MARPE effects to be observable in photoemission from any solid surface, with strength depending on the relative intensities of the absorption resonances. Furthermore, for homogeneous systems with flat surfaces, the x-ray optical model should provide a reasonably quantitative picture of the observed phenomena. Effects following an x-ray optical analysis have also recently been observed for photoemission from an adsorbate on a metal-N_2/Ni(001) [10]. For more complex cases with, e.g., three-dimensional nanometer-scale heterogeneity, the use of a microscopic model will be more appropriate.

SF_6: In Figure 2, experimental results for SF_6 are summarized. The x-ray absorption coefficient is shown in Figure 2(b), and the S 2p photoemission intensity and its asymmetry parameters were measured as photon energy was scanned across the "A" absorption resonance (corresponding to a F

1*s* t_{1u}-to-a^*_{1g} excitation). Although the total S 2p intensity (proportional to σ) does not show a significant change in crossing the resonance (≤few %), the dipole asymmetry parameter β (as shown in Figure 2(b)) exhibits about a 15% excursion in magnitude that is also of the same general form as those in Figure 1. Similar effects are also seen in the parameters δ and γ [11].

Thus, interatomic resonant effects are also seen in this free molecule, and although they are too small to be observed as yet in the total intensity, they are clearly observed in the various asymmetry parameters. No theoretical calculations have as yet been performed for this case, but the x-ray optical model would clearly be inappropriate, and a microscopic approach such as that discussed previously [3,5] is the logical starting point for understanding these effects.

CONCLUSIONS

Multi-atom resonant photoemission effects are found in both the total intensities from homogeneous solid surfaces and adsorbates on such surfaces, for which an x-ray optical model is found to well describe the data, and in the angular distribution asymmetry parameters of a free molecule, for which a microscopic theoretical approach will be necessary. Similar effects in nanoscale structures will lie somewhere between these two cases.

REFERENCES

1. A. Kay, E. Arenholz, B.S. Mun, F.J. Garcia de Abajo, C.S. Fadley, R. Denecke, Z. Hussain, and M.A. Van Hove, *Science* **281**, 679(1998).
2. (a) E. Arenholz, A.W. Kay, C.S. Fadley, M.M. Grush, T.A. Callcott, D.L. Ederer, C. Heske, and Z. Hussain, *Phys. Rev. B* **61**, 7183 (2000); (b) E. Arenholz, A.W. Kay, unpublished results.
3. F.J. Garcia de Abajo, C.S. Fadley, and M.A. Van Hove, *Phys. Rev. Lett*. **82**, 4126 (1999).
4. A.W. Kay, Ph.D. dissertation (University of California-Davis, September, 2000), Chapters 4 and 5.
5. A.W. Kay, F.J. Garcia de Abajo, S.H. Yang, E. Arenholz, B.S. Mun, M.A. Van Hove, Z. Hussain, and C.S. Fadley, Physical Review B **63**, 5119 (2001).
6. A. Kikas, E. Nommiste, R. Ruus, A. Saar, and I. Martinson, Sol. St. Commun. **115**, 275 (2000).
7. (a) M.G. Garnier, N. Witkowski, R. Denecke, D. Nordlund, A. Nilsson, M. Nagasono, and N. Mårtensson, and A. Föhlisch, Maxlab Annual Report for 1999 and private communication correcting this data; (b) D. Nordlund, M. G. Garnier, N. Witowsky, R. Denecke, A. Nilsson, M. Nagasono, N. Mårtensson and A. Föhlisch, Phys. Rev. B **63**, 121402 (2001).
8. M. Finazzi, G. Ghiringhelli, O. Tjernberg, L. Duo, A. Tagliaferri, P. Ohresser, and N. B. Brookes, Phys. Rev. B **62**, R16215 (2000).
9. (a) O. Hemmers et al., Rev. Sci. Instrum. **69**, 3809 (1998); (b) O. Hemmers et al., Phys. Rev. Lett. **87**, 273003 (2001).
10. D. Menzel, W. Wurth, A. Föhlisch, P. Fuelner, S.-H. Yang, and C.S. Fadley, private communication.
11. H. Wang, O. Hemmers, P. Focke, M. M. Sant'Anna, D. Lukic, C. Heske, R. C. C. Perera, I. Sellin, and D. Lindle, to be published.

This work was supported by the U.S. Department of Energy, Office of Science, Office of Basic Energy Sciences, Materials Sciences Division, under Contract No. DE-AC03-76SF00098, and the National Science Foundation.

Principal investigator: N. Mannella, Department of Physics UC Davis, and Materials Sciences Division, Lawrence Berkeley National Laboratory. Email: norman@electron.lbl.gov. Telephone: 510-486-4581

Figure 1. (a) Experimental geometry for measurements on Ni(001). (b)-(f) O 1s intensity as photon energy is scanned through the Ni $2p_{1/2\text{-}3/2}$ absorption resonances. Both experimental data (blue points) and theoretical calculations based on an x-ray optical model (red curves) are shown.

Figure 2. (a) Experimental geometry for measurements on gas-phase SF_6. (b) The x-ray absorption coefficient in the F 1s region as measured by partial electron yield. (c) The dipole asymmetry parameter β as photon energy is scanned through the "A" resonance in (b).

Figure 1.

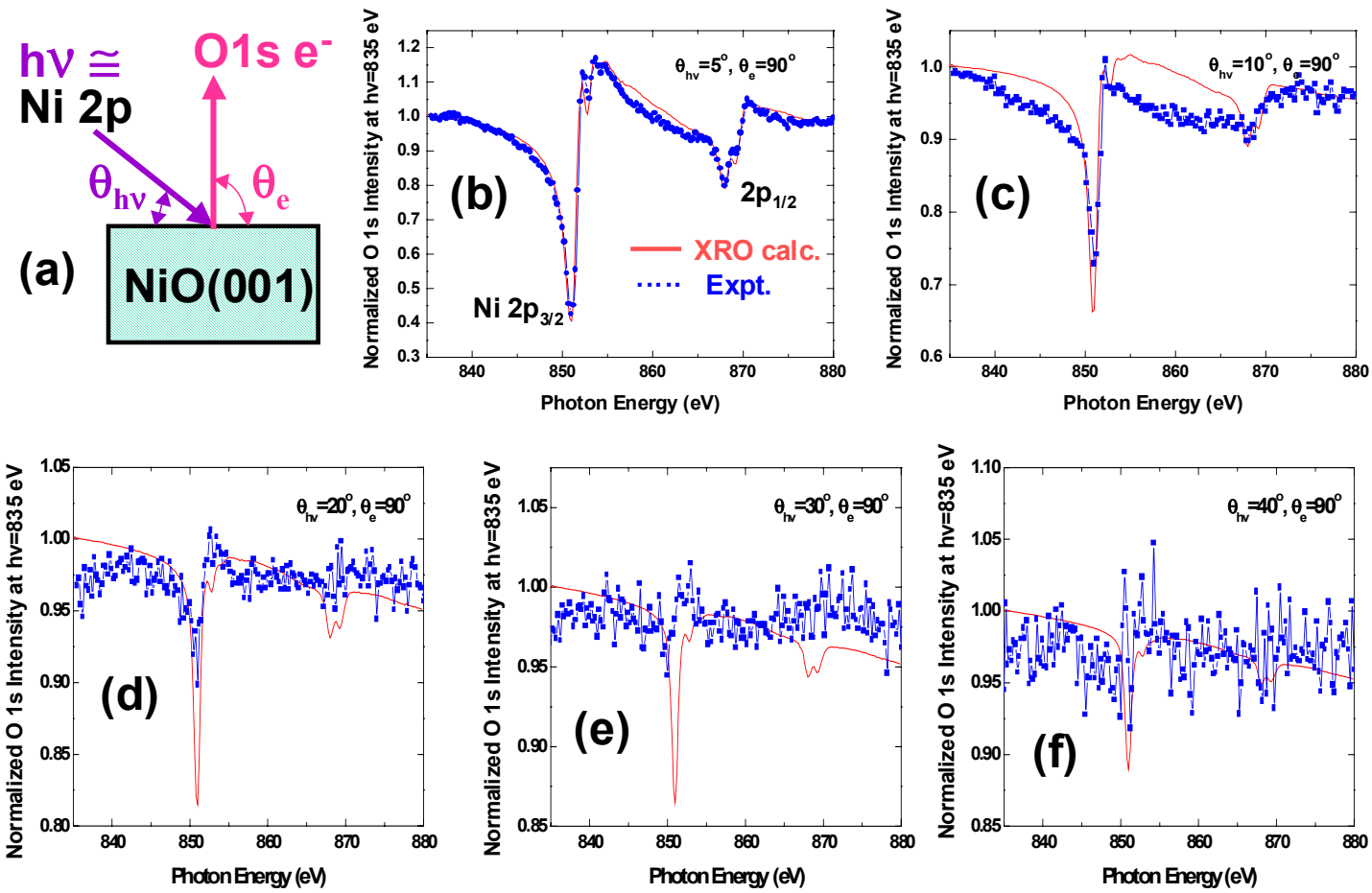

Figure 2.

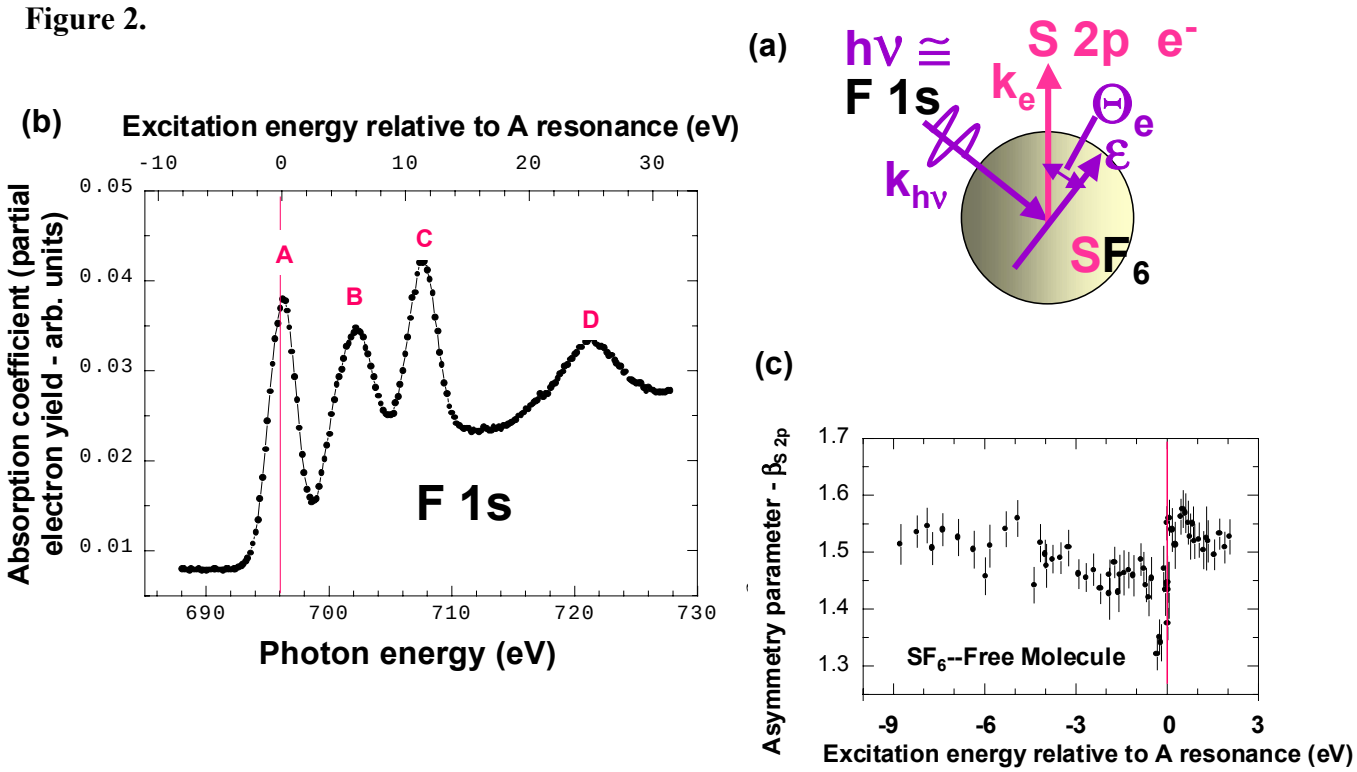

SHALLOW AND DEEP CORE LEVEL IONIC FRAGMENTATION OF THE CCl_4 MOLECULE

A. C. F. Santos[1] , J. B. Maciel[1] , M. M. Sant'Anna[2], K. T. Lung[4] , J. Cotter [5], W. Stolte[3] , and G. G. B. de Souza[1]

[1]Instituto de Química, Universidade Federal do Rio de Janeiro, Brazil
[2]Pontifícia Universidade Católica do Rio de Janeiro, Brazil
[3]Advanced Light Source, Berkeley, CA, USA
[4]University of Waterloo, Canada
[5]University of Nevada, Reno, USA

Carbon tetrachloride, CCl_4, is a volatile compound with several important technological applications, being for instance used as an etching agent in microelectronics. In addition, the CCl_4 molecule pollutes atmosphere harmfully and has been related to the so-called greenhouse effect [4]. Several studies have been dedicated to the photoabsorption spectrum of the CCl_4 molecule, both in the valence and inner-shell regions [1-4]. This molecule presents a tetrahedral symmetry (T_d point group).

In this work we report on the ionic fragmentation of the CCl_4 molecule following valence, and core level photoexcitation, using tunable synchrotron radiation as exciting source. Branching ratios for the ionic fragments have been determined, as a function of the incident photon energy around the valence, Cl 2*p* edge (~200 eV)., C 1*s* continuum (~ 300 eV), and Cl 1s (~ 2800 eV) regions.

The valence and shallow core levels (Cl 2p and C 1s) measurements were performed at the Center for Advanced Microstructures and Devices (CAMD), Louisiana, USA. The experimental set up has been described recently [5]. Basically, light from a toroidal grating monochromator (TGM) beamline intersected an effusive gaseous sample inside a high vacuum chamber, with base pressure in the 10^{-8} torr range. PEPICO and PIPICO data were determined as a function of the photon energy using a time-of-flight mass spectrometer.

The second part of this work (deep core level ionization) was performed using x-ray synchrotron radiation from beamline 9.3.1 at the Advanced Light Source (ALS) in Berkeley, California. 9.3.1 is a bending magnet beamline covering 2-6 keV photon-energy range. This beamline provides a flux of 10^{11} photons s^{-1} in a bandpass $\leq$ 0.5 eV. Photon-energy calibration was achieved by scanning the monochromator through the Cl K-edge region while monitoring the total-ion yield . The photon-energy was determined with 0.2 eV accuracy. Figs. 1 and 2 show the PEPICO mass spectra of CCl_4 around the Cl 2p and Cl 1s edges.

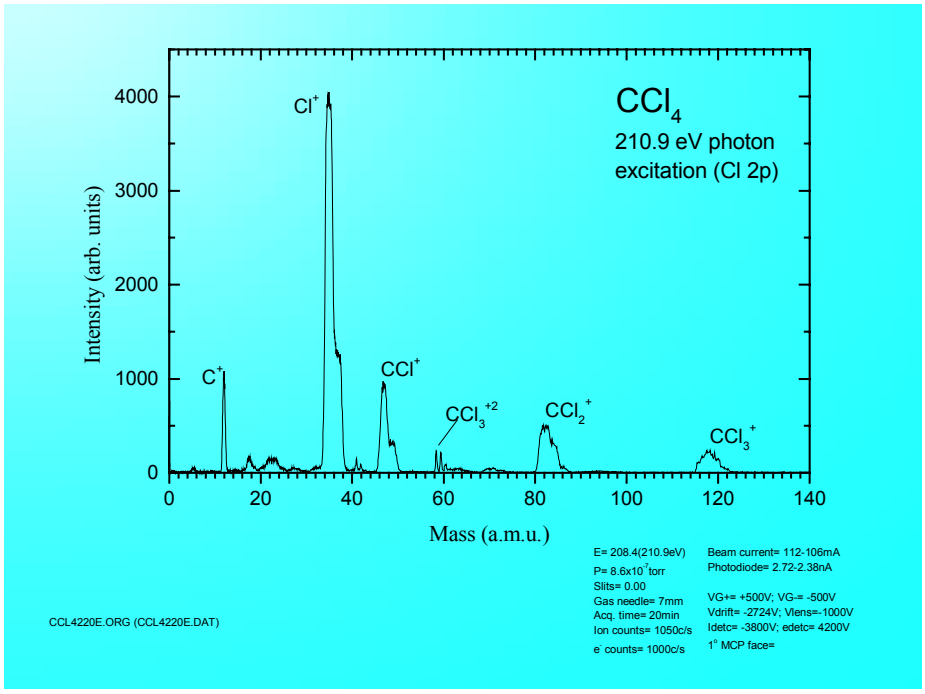

Fig 1. - Mass Spectrum of CCl_4 molecule near the Cl 2p edge (210 eV).

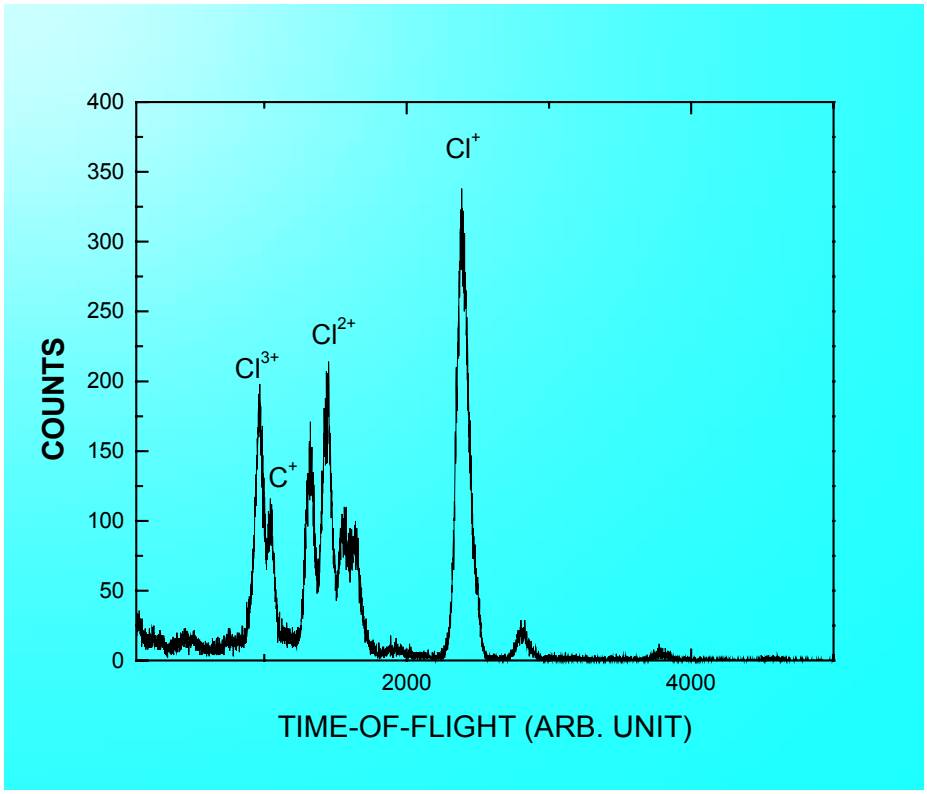

Fig.2 – Mass spectrum of CCl_4 molecule around Cl 1s edge.

There is no evidence for stable CCl_4^+ ion in the energy range studied in this work in accordance with earlier studies using electron impact technique [6, 7]. The first evidence for metastable CCl_4^+ ion was given by Drewello *et al.* [8], with lifetimes in the order of 10^{-5} s. According to Kaufmann *et al.* [8], the CCl_4^+ is not observed because the excitation of the carbon tetrachlorine molecule occurs into a repulse excited state of neutral CCl_4 which dissociates into Cl and CCl_3 that in turns, autoionizes giving rise to CCl_3^+ ion. Leiter *et. al.* [6] observed the metastable dissociation of CCl_4^{+*} into CCl_3^+ and Cl, avoiding the postulation of dissociation of neutral CCl_4 prior to ionization.

The authors would like to thank the CAMD and ALS staffs for the very efficient operation of the respective synchrotron rings. They also would like to express their gratitute to Prof. Fred Schlater (ALS) and C. Cisneros (UNAM) for support. We also acknowledge Prof. D. Lindle for the use of a vacuum chamber. Three of the authors (A.C.F.S., J.B.M. and G.G.B.de S.) are indebted to FAPERJ and CNPq (Brazil) for financial assistance.

References:

1 – A. P. Hitchcock and C. E. Brion, Journ. Electr. Spectr. Rel. Phen., **14** (1978) 417-441.
2 – W. Zhang, T. Ibuki, and C. E. Brion, Chem. Phys. **160** (1992) 435-450.
3 – G. O'Sullivan, J. Phys. B. At. Mol. Opt. Phys. **15** (1982) 2385-2390.
4– G. R. Burton, W. F. Chan, G. Cooper and C. E. Brion Chem. Phys. **181** (1994) 147-172.
5- A.C.F. dos Santos, C.A.Lucas and G.G.B. de Souza, J.El.Spectr. and Rel. Phen., **114-116** (2001) 115-121.
6- K. Leiter, K. Stephan, E. Märk, and T. D. Märk, Plasma Chemistry and Plasma Processing, **4**, (1984) 235-249.
7- R. F. Baker and J. T. Tate, Phys. Rev. **53**, 683 (1938).
8- T. Drewello, T. Weiske, and H. Schwarz, Angew. Chem. Int. Ed. Engl. **24,** 869 (1985).

Principal investigator: Gerardo Gerson B de Souza, Instituto de Química, Universidade Federal do Rio de Janeiro. E-mail: gerson@iq.ufrj.br. Telephone: (55) 021 2590-9024.

Soft x-ray emission spectroscopy of ions in solution

A. Augustsson[1], J.-H. Guo[1,3], D. Spandberg[2],
K. Hermansson[2] and J. Nordgren[1]

[1]Department of Physics, Uppsala University, Box 530, S-75121 Uppsala, Sweden
[2]Department of Materials Chemistry, Uppsala University, P.O. Box 538, S-75121, Uppsala, Sweden
[3]Advanced Light Source, Ernest Orlando Lawrence Berkeley National Laboratory, University of California, Berkeley, California 94720, USA

INTRODUCTION

Metal-ion transport in both aqueous- and polymer-solvent media involves continuos solvent-ligand exchange. Metal-ion coordination chemistry is therefore fundamental to these phenomena. The application of soft-x-ray absorption spectroscopy (SXAS) and soft-x-ray emission spectroscopy (SXES) to study wet samples has been hampered by the experimental difficulties of handling wet samples under high-vacuum conditions. Optical, infrared and Raman spectroscopies as well as magnetic resonance based methods are often used to determine the structure and the properties of these systems [1]. Here, we report the soft x-ray absorption and emission study of cations (Li^+, Na^+, K^+, Mg^{2+}, and Al^{3+}) in water solution.

Experiment

The experiments were performed at beamline 7.0.1 at the Advanced Light Source (ALS), Lawrence Berkeley National Laboratory. The beamline comprises a 99-pole, 5 cm period undulator and a spherical-grating monochromator [2]. In the liquid phase measurements, the incident photon beam and secondary emission penetrated a thin silicon nitride window of 100 nm in thickness. XAS spectra of liquid water were recorded in x-ray fluorescence yield. XES spectra were recorded using a high resolution grating spectrometer [3].

Cation-solvent interaction

The solvated cation interaction can be monitored by examining the spectra of the solvent. The advantage of this approach is that the restriction to cations no longer applies. For example, it can be used in studying what happens when salts of the alkali and alkaline earth metals are added to aqueous solvent. Series of spectra at different salts at a given concentration exhibit an isosbestic point. In the figure experimental data

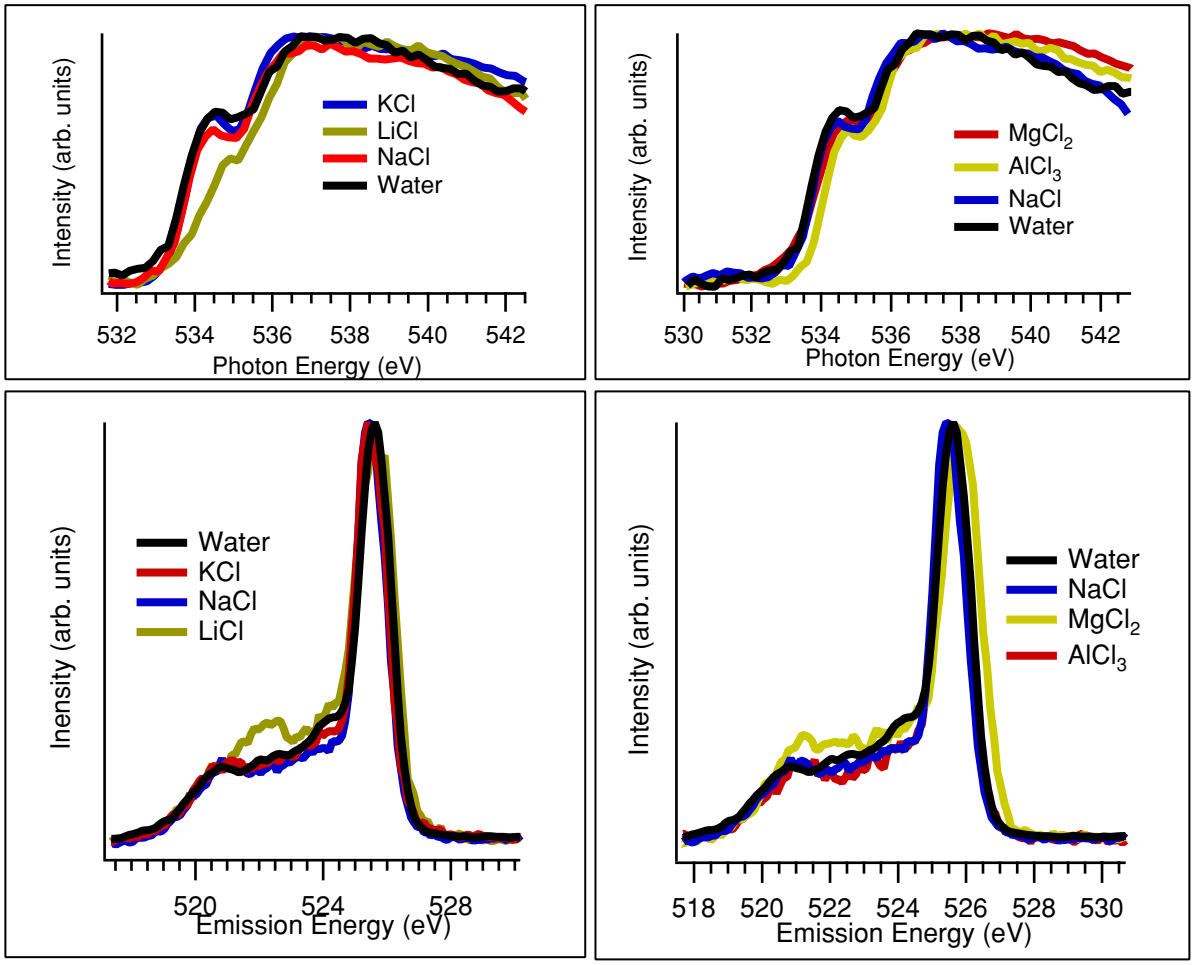

Figure 1: Top panels, O 1s XAS spectrum and bottom panels resonant O K-emission spectra of Ion solutions exited at the photon energy 534.5 eV

from ion-solutions are presented. Spectrum of pure water is also presented for comparison. The bottom panels shows the resonantly excited x-ray emission spectra, excited on the pre-edge in the absorption spectra at $\sim$ 534.5 eV (top panels). The left panel shows a comparison of O 1s spectra of solutions with ions of varying sizes and the right panel shows spectra varying charge. In the emission spectra one observe that spectrum of Na^+ and Al^{3+} solutions are similar while the emission spectrum of the Mg^{2+} solution show a broadened main peak, and some distinct differences at lower energies. Comparing Na^+ and K^+ solutions a small difference is observed, while the smaller Li ion shows a large spectral effect both in absorption and emission. We are presently working with theoretical interpretation, to achieve a full understanding of the data.

References

[1] Jean-Joseph Max and Camille Chapados, J. of Chem. Phys., 115, (2001), p. 2664

[2] T. Warwick and P. Heimann and D. Mossessian and W. McKinney and H. Padmore, Rev. Sci. Instrum. , 66, (1995), p.2037

[3] J. Nordgren and G. Bray and S. Cramm and R. Nyholm and J. -E. Rubensson and N. Wassdahl, Rev. Sci Instum. , 60, (1989), p.1690

This work was supported by the Swedish Research Council (VR), the Göran Gustafsson Foundation for Natural Science and Medicine, and the Swedish Institute.

Principal investigator: E. Joseph Nordgren, Department of physics, Uppsala University, Email: joseph@fysik.uu.se. Telephone: +46 18 4713554.

Spin-Resolved Electron Spectroscopy of Carbonyl Sulphide

G. Turri[1,2], G. Snell[1], B. Langer[3], M. Martins[4], E. Kukk[5], P. Langhoff[6,7,8] and N. Berrah[1]

[1]Western Michigan University, Department of Physics, Kalamazoo, MI 49008, USA
[2] Lawrence Berkeley National Laboratory, Advanced Light Source division, Berkeley, CA 94720, USA
[3] Fritz-Haber-Institut der Max-Planck-Gesellschaft, 14195 Berlin, Germany
[4] Freie Universität Berlin, Institut für Experimentalphysik, 14195 Berlin, Germany
[5] Dept. of Physics, Oulu University, 90570 Oulu, Finland
[6] Air Force Research Laboratory, AFRL/PRS, Edwards AFB, California 93524-7680
[7] Department of Chemistry, Indiana University, Bloomington, Indiana 47405
[8] San Diego Supercomputer Center, University of California, 9500 Gilman Drive, La Jolla, California 92093-0505

Introduction

Energy- and angle-resolved photoelectron spectroscopy has been widley used to investigate the structures of atoms, molecules and solid matter as well as the dynamics of photoemission processes. Though, the information that can be obtained with this technique is often incomplete, even when the most simple systems are investigated [1]. Quantum mechanically the photoemission process is described in terms of the wavefunctions for the initial and final states and the Coulomb or dipole transition matrix elements. The determination of all the matrix elements of one physical process is the aim of the so-called complete (or perfect) experiment [2,3]. This definition is clearly model dependent [3].

Different techniques have been introduced to tempt a complete photoionization experiment. Some make use of coincidence between electron and electron [4,5,6] , or electron and fluorescent photon [7,8]. Other take advantage of the properties of polarized atoms [9,10]. The possibility of using spin-resolved electron spectroscopy has been theoretically described by Huang for photoionization [11] and Auger decay [12]. Since then, this technique has been widley used in experiments, see [13,14,15] for example.

Despite the substantial advancements of complete experiment in atomic systems, there have been only very few studies of inner-shell photoionization of molecules beyond intensities and angular distributions [16]. A molecular complete experiment is much more difficult than the determination of matrix elements for atoms, because of the large number of possible outgoing partial waves. Additionally, the molecular environment can influence the core orbitals of the atoms in the molecule. This can lead to the splitting of energy levels due to vibrations, lower than spherical symmetry of the system, etc.

In this work we report on spin polarization measurements of the sulphur 2p photoionization of carbonyl sulphide molecule. Recently, Kukk et al. [17] investigated the sulphur 2p photoionization of OCS molecules by high-resolution, angle-resolved electron spectroscopy. They found that the angular distribution parameter β of the two molecular-field-split components of the sulphur $2p_{3/2}$ line differs significantly at a broad range of photon energies above the 2p threshold. Since the origin of this difference cannot be traced solely by angle-resolved spectroscopy, we measured the spin polarization of the S 2p lines. The analysis of the acquired data is still in progress; some preliminary results will be presented here.

Experiment

The experiment was performed at Beamline 4 at Advanced Light Source (ALS) storage ring. We used circularly and linearly polarized light from the new elliptical polarization undulator (EPU) [18]. The sulphur 2p photoionization was measured for 6 different photon energies, namely 185, 191, 195, 205, 220 and 260 eV. With the chosen setting of the parameters of the beamline, a photon flux of approximately 10^{14} photons/sec and a resolving power $E/\Delta E$

about 1000 was provided. The degree of both circular and linear polarization for all the photon energies was 100% within the experimental errors. The photon beam crossed perpendicularly an OCS effusive gas jet. The kinetic energy of the photoemitted electrons was measured with two Time Of Flight (TOF) spectrometers. Combined with one of the TOF, a spherical Mott polarimeter of the Rice type, operated at 45KV, performed the spin polarization analysis. The instrumental asymmetry of the Mott polarimeter was accounted by combining measurements with positive and negative light helicity [19], changing polarization approximately every 10 min. Due to the substantial loss of signal intensity during the Mott scattering, our experiment considerably benefited from the TOF technique's inherent capability of simultaneous acquisition of all lines in the spectrum.

Results

The sulphur 2p-photoionization spectrum of OCS, as measured with 205 eV circularly polarized photon, is reported in the lower panel of Fig.1 (sum of the spectra with different spin polarization).

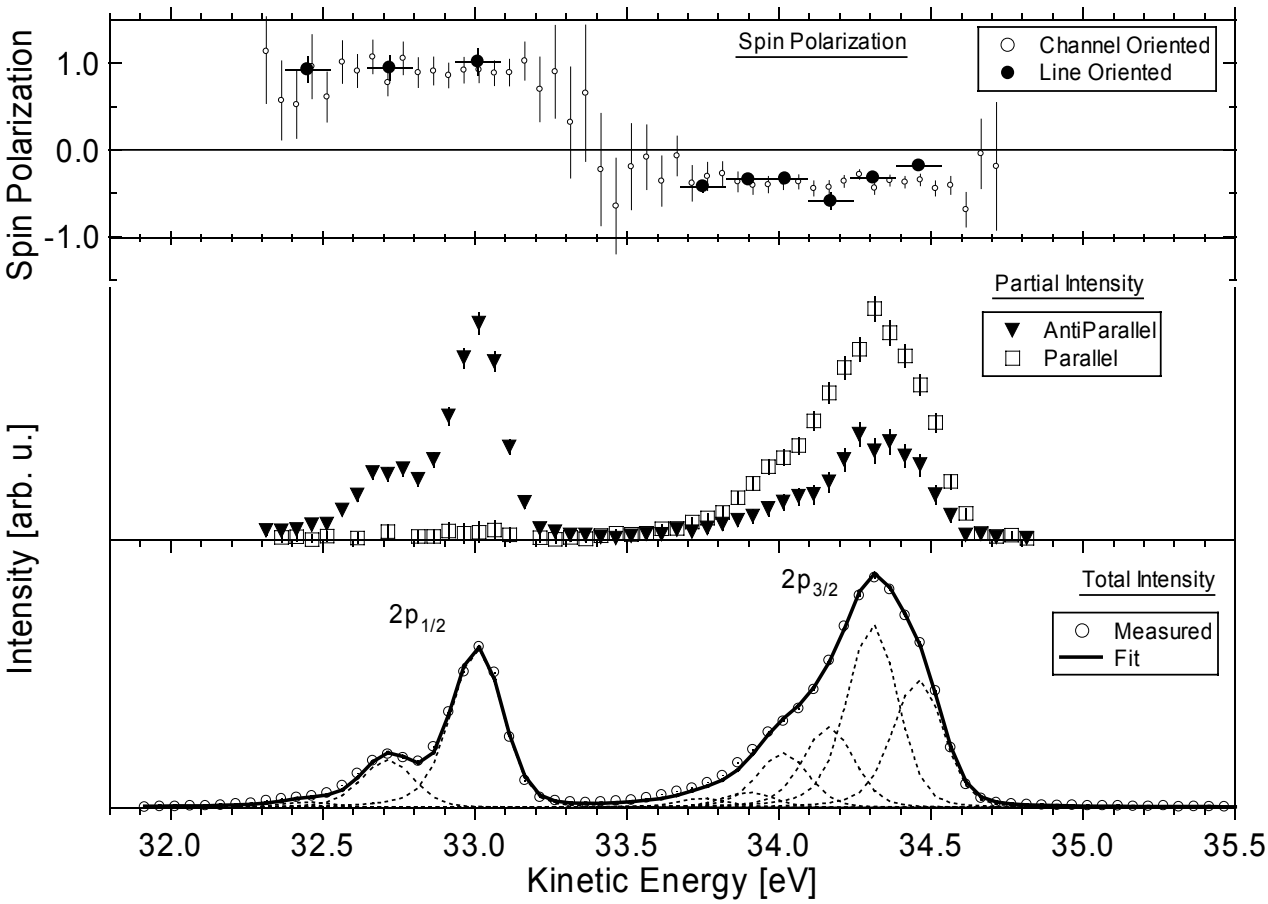

Fig.1: Sulphur 2p-photoionization spectrum of OCS molecule, as measured with 205 eV circularly-polarized photon. (bottom) Total Intensity, the continuous curves are the result of a least-squares fitting procedure. (middle) Spin-Separated Intensity. (up) Spin Polarization. See text for details.

As described in details by Kukk et al. [17] the spectrum can be completely understood in terms of spin-orbit, vibrational and molecular field split. Within the resolution of our experiment, the two spin-orbit components are easily resolved; in order to solve the vibrational and molecular field splitting, we applied a least-squares fitting procedure, using asymmetric Voight profiles.

We applied two different techniques to extract the spin polarization from our data. The areas of

the different peaks, as returned by the fitting procedure, were used to obtain the polarization of the different components of the spectrum. This technique has been referred as a "Line-Oriented" analysis [15]. Alternatively, we applied a "Channel-Oriented" analysis, where the spin polarization has been calculated for each point of the photoemission spectra. The results of the two methods are reported in the top panel of Fig.1, showing good agreement. Using the values obtained with the latter analysis, we deduced the spin separated spectra [14], which correspond to the spectra that a "perfect" Mott polarimeter (i.e. with no instrumental asymmetry, and Sherman function equal to1) would measure in case of completely circularly polarized light. These spectra are reported in the middle panel of Fig.1.

Both the spin-orbit components show strong spin-polarization. Conversely, the vibrational and the molecular splitting show minor effect on the spin polarization at this photon energy. The polarization of the three states of the $2p_{1/2}$ peak is $+0.95 \pm 0.15$, i.e. these states are almost completely spin-polarized. This is reflected in the vanishing of the $2p_{1/2}$ peak in the spin separated spectrum associated with electron spin parallel to the photon spin. The states associated with the $2p_{3/2}$ peak show slightly different polarization values out of the error bars. The different sign in the spin polarization of the two spin-orbit states qualitatively agree with the fact that the polarization of the 2p photoionization line should vanish when the spin-orbit structure is not resolved.

Conclusion

Whereas the most of the analysis has to be done, the few preliminary results seem to be encouraging. The investigated transitions show strong spin polarization, which makes them very suited for spin resolved technique. The agreement of the results obtained by using different analysis techniques confirms the consistency of the investigation.

Funding

Department of Energy, Office of Science, Basic Energy Sciences, Chemical Sciences Division

References

[1] B. Schmidtke et al., J. Phys. B **33**
[2] U. Heinzmann et al., J. Phys. B **13**, 4353 (1980).
[3] J. Kessler et al., Comments At. Mol. Phys.**10**, 47 (1981).
[4] N.M. Kabachnik et al., J. Phys.B **32**, 1769 (1999).
[5] K. Ueda et al., Phys. Rev. Lett. **83**, 5463 (1999).
[6] G. Turri et al., J. Elect. Spect. **114**, 199 (2001).
[7] J. Jimenez et al., Phys. Rev. Lett. **57**, 2260 (1986).
[8] H.-J. Beyer et al., J. Phys. B **28**, L47 (1995.)
[9] O. Plotzke et al., Phys. Rev. Lett. **77**, 2642 (1996.)
[10] K. Godehusen et al., Phys. Rev. A **58**, R3371 (1998).
[11] K.-N. Huang, Phys. Rev. A **22**, 223 (1980).
[12] K.-N. Huang, Phys. Rev. A **26**, 2274 (1982).
[13] G. Snell et al., Phys. Rev. Lett. **82**, 2480 (1999).
[14] U. Hergenhahn et al., Phys. Rev. Lett. **82**, 5020 (1999).
[15] G. Snell et al., Phys. Rev. A **63**, 032712 (2001).
[16] E. Shigemasa et al., Phys. Rev. Lett. **80**, 1622 (2000).
[17] E. Kukk et al., J. Phys. B **33**, L51 (2000)
[18] A.T. Young et al., Nuc. Instrum. and Methods A **467**, 549 (2001)
[19] T.J. Gay and F.B. Dunning, Rev. Sci. Instrum. **63**, 1635 (1992)

Principal investigator: Nora Berrah, Physics Department, Western Michigan University, Kalamazoo, MI 49008.
Telephone: (1) 616-387-4955. Fax: (1) 616-387-4939. Email: berrah@wmich.edu.

Vibrationally resolved resonant Auger spectroscopy of formaldehyde at the C$1s^{-1}\pi^*$ resonance.

J.D. Bozek[1], S.E. Canton[1,2], E. Kukk[3] and N. Berrah[2]
[1] Lawrence Berkeley National Laboratory, Advanced Light Source, University of California, Berkeley CA 94720.
[2] Department of Physics, Western Michigan University, Kalamazoo MI 49008.
[3] Department of Physical Sciences, Oulu University, Linnanmaa, Oulu FIN-90570, Finland.

INTRODUCTION

Resonant Auger (RA) spectroscopy has benefited greatly from advances in both light sources and electron spectrometer techniques in the past decade. Transitions to molecular orbitals are particularly interesting to study using RA spectroscopy due to the dynamics induced in the excited state. When it is not dissociative, changes in the molecular geometry induced by the excitation allow the RA decay process to sample different parts of the potential energy surface of the molecule that can not be accessed directly by single photon absorption and extensive vibrational structure is often observed in the participator decay. Such studies have been performed with vibrational resolution for a number of simple diatomic or triatomic [1,2] molecules and start being explored for larger molecules. In this work, vibrationally resolved RA spectra of gaseous formaldehyde have been measured under resonant Raman conditions at several photon energies on the C$1s^{-1}\pi$ resonance. Utilizing high-resolution photoexcitation, specific vibrational states of the C$1s^{-1}\pi^*$ resonance were selectively populated. Participator Auger decay of the excited state populates mainly the A-D ionic states, without any discernable increase in the intensity of the X state. The vibrational manifold of the A state band was examined in details for resonant and non-resonant photoionization. The observations are attributed to changes in the potential energy surfaces.

EXPERIMENT

The experiments were carried out on beamline 10.0.1, which delivers more than 10^{12}photons/sec in 0.1% bandwidth. The photoelectron spectra were measured with a GammaData Scienta SES-200 hemispherical analyzer in a spectrometer system developed exclusively for gas phase experiments. Monomeric formaldehyde in the gas phase was obtained by heating to 70^0C the sample cell containing the dimerized form paraformaldehyde (Aldrich, 96% purity). The presence of monomeric formaldehyde and its purity were verified by measuring the outer valence photoelectron spectrum.

RESULTS

A low-energy electron yield spectrum of the C$1s^{-1}\pi^*$ resonance shown in Fig.1 was first measured with the present apparatus to provide good calibration of the energy scale for the subsequent RA measurements. This spectra gives also an idea of the extent of excitation for each normal mode ν_1 mostly C-H stretching, ν_2 C=O mostly stretching, ν_3 mostly HCH bending (Table 1). Vibrationally resolved RA spectra were recorded at the energies corresponding to the positions indicated on Fig.1.and are shown of Fig.2. RA spectra a-c were measured at photon energies corresponding to the excitation of primarily ν_2 quanta in the excited state. The position of the peak intensity steadily increases through higher vibrational levels in the ionic state as higher ν_2 vibrational levels are accessed in the core excited state. The trend continues for spectra d-f although the vibrational levels populated in the excited state become less clear due to the probability of exciting mixtures of quanta ν_1 and ν_3. This behavior can be qualitatively explained: the change from spectrum a to c is mainly due to the excitation of the higher levels of the ν_2 manifold of the A state, as the vibrational transitions originate from the ν_2=0,1,2 levels of the core excited state respectively. Consequently, the maximum intensity shifts from the ν_2=0 (spectrum a) to the ν_2=2 level (spectrum c) of the final ionic state A. The spectrum has quite different appearance, as now the vibrational transitions originate from the ν_1=1 level, but the ν_2=2 manifold again comes from the ground level of the core excited state (as for spectrum a). Thus the ν_2=0 final state is again populated strongly, but the intensity is shifted to the higher levels in the ν_1 final state manifold. The next spectra e and f again display changes due to the intensity moving to the higher levels of the manifold. The vibrational states populated in the B state band are less obvious owing to the band's lower intensity, but similar trends are discernable. The dispersion of the vibrational intensity A and B state can be attributed to geometric changes in the potential energy surfaces (PES). Geometric changes in the H_2CO molecule upon excitation were reported by analysis of photoabsorption spectrum [3]. The C=O bond increases, while the

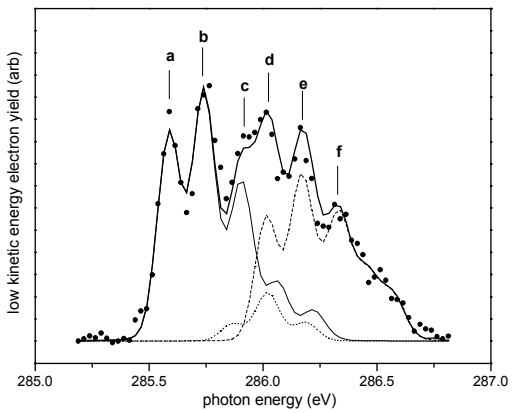

FIG.1 : Low energy electron yield of the $C1s^{-1}\pi^*$ resonance in formaldehyde measured with 75 meV photon resolution. The experimental data has been deconvoluted into contributions from different vibrational states using parameters from [3]. The positions where resonant Auger spectra were measured are indicated by the letters a-f.

C-H bond contracts. The A RA final state, results from the removal of a C=O bond in the ionic state and as such, the resonant decay occurs between two states with similarly displaced PES. Hence the ν_2 vibrational quantum number of the excited state is preserved in the ionic state and reflected in the vibrational populations in the participator Auger decay lines. The ν_1 progression is very strong, however, indicating that there is a large change in the C-H bond distance between the core excited and A ionic state

TABLE 1: Photon energies of the positions indicated of Fig. 1,where resonant Auger spectra were measured, and relative contributions of different vibrational levels to the $C1s^{-1}\pi*$ band at those energies.

Label	Photon Energy	Vibrational State Contribution (total = 100)
a	285.59	(0,0,0) – 100
b	285.74	(0,1,0) – 100
c	285.89	(0,2,0) – 82 (0,0,1) – 10 (1,0,0) – 8
d	286.02	(1,0,0) – 52 (0,1,1) – 20 (0,3,0) – 14 (0,4,0) - 14
e	286.17	(1,1,0) – 76 (0,4,0) – 8 (0,5,0) – 8 (0,2,1) – 8
f	286.32	(1,2,0) – 78 (1,0,1) – 14 (1,1,1) – 8

REFERENCES

[1] Kukk et al, Phys. Rev. A **62** (2000) 032708/1-9
[2] Miron et al J. Electron Spectrosc. Relat. Phenom. **93**, 95 (1998)
[3] Remmers et al, Phys. Rev. A **46**, 3945 (1996)

This work was funded by the Department of Energy, Office of Science, Basic Energy Sciences, Chemical and Material Science Division, under the contract No. DE-AC03-76SF00098.

Principal investigator: Nora Berrah, Physics Dept., Western Michigan University, 616-387-4955, berrah@wmich.edu.

ACKNOWLEDGEMENTS

We are indebted to Bruce Rude for his outstanding technical assistance and the staff of the ALS for their excellent operation of the facility.
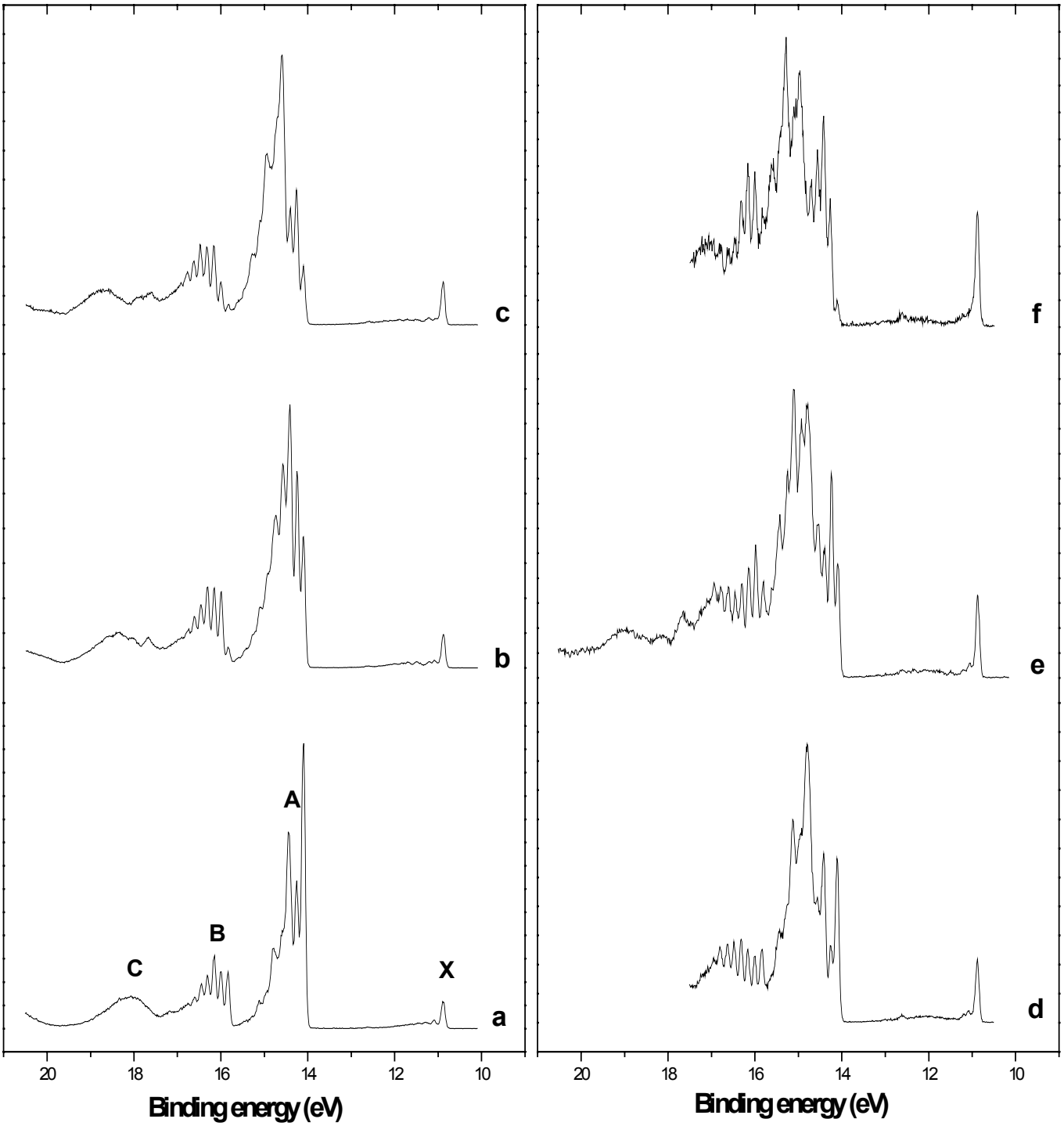
FIG. 2 : Vibrationally resolved resonant Auger spectra of the participator decay states of formaldehyde measured at the positions indicated on Fig.1 and in Table1.